

K 55161

AIR MINISTRY  
For Official Use

R. & M. No. 1675

AERONAUTICAL RESEARCH COMMITTEE  
REPORTS AND MEMORANDA No. 1675  
(T.3602)

# Graphical Method of Calculating Performance of Airscrew

By **C. N. H. LOCK**  
M.A.

OCTOBER, 1934

*Crown Copyright Reserved*



LONDON

PRINTED AND PUBLISHED BY HIS MAJESTY'S STATIONERY OFFICE  
To be purchased directly from H.M. STATIONERY OFFICE at the following addresses:  
Adastral House, Kingsway, London, W.C.2 ; 120 George Street, Edinburgh 2 ;  
York Street, Manchester 1 ; 1 St. Andrew's Crescent, Cardiff ;  
80 Chichester Street, Belfast ;  
or through any Bookseller

1935

Price 2s. 6d. Net

R  
5

3 8006 10054 8745

A GENERAL METHOD OF CALCULATING THE  
PERFORMANCE OF AN AIRSCREW

---

By C. N. H. Lock, M.A., of the Aerodynamics Department, N.P.L.

---

*Reports and Memoranda No. 1675*

25th October, 1934

*Summary.*—A rapid method is described of making calculations of airscrew performance by means of charts. The first application is to ordinary strip theory calculations on the basis of the formulae of Ref. 5. Six charts are required for each radius for which the value of thrust grading, etc., are to be derived; of these six, four depend on number of blades but are otherwise universal, since they are independent of shape of blade section, and do not involve the blade width or blade angle explicitly; they are based purely on the application of Prandtl theory to the airscrew and contain no empirical adjustments. The remaining two charts involve the lift and drag curves of the section.

The second application gives a considerable further simplification in that the charts are required for a single standard radius (0·7) only; the thrust coefficient corresponding to a given working condition can then be deduced by a simple operation with three charts while the torque involves three further charts and a simple addition. The accuracy of the second method is increased if the lift and drag charts are deduced by analysis of observations on (model) airscrews, an analysis which can be performed rapidly by means of the remaining four charts; such an analysis of the results of the "wind tunnel tests of high pitch airscrews"<sup>4</sup> shows that the method will give reasonably consistent results over a range of pitch ratio from 0·3 to 2·5, while there is little doubt that the method will cover the range of blade width likely to occur in practice. Changes of blade section and also of plan form and twist may be included if necessary by modifying the lift and drag curves. The second method has also been remarkably successful in its application to the stalled range of an airscrew, a range in which there is at present no other available method.

It is further suggested that the first method might prove very convenient for analysing wind tunnel tests of model airscrews at high tip speed; the accuracy of application of the second method might be improved by basing the lift curves on full scale values of power, speed and revolutions, combined with an estimate of profile drag.

*Note.*—For practical use the necessary charts should be plotted on a fairly large scale from the tables given in the report; e.g., Chart 1 should be a transparency measuring at least 22 in. × 15 in. The small scale charts given in the report are intended for illustration only.

---

## LIST OF SYMBOLS

(cf. also list of symbols in Ref. 5.)

- $\theta$  = Blade angle. }  
 $\alpha$  = Blade incidence. } Fig. 1. (p. 4).  
 $\phi = \theta - \alpha.$  }  
 $\phi_0$  §2, Equation 2, and Fig. 1.  
 $\beta = \phi - \phi_0.$  Fig. 1.  
 $W$  = Resultant velocity relative to a blade element. Fig. 1.  
 $w_1$  = Total interference velocity. Fig. 1.  
 $\Omega$  = Angular velocity, radians per second.  
 $r$  = Radius of blade element.  
 $R$  = Tip radius.  
 $x = r/R.$   
 $\kappa$  = " Tip loss coefficient " Ref. 5, §2.  
 $s$  = Solidity =  $Nc/2\pi r.$   
 $N$  = Number of blades.  
 $c$  = Blade chord.  
 $k_L, k_D$  = Lift and drag coefficients of blade element (two dimensional flow).  
 $k_{L_0} = k_L - sk_D \tan \phi$  (above the stalling angle).  
 $w_c$  §2, Equation (6).  
 $W_c$  §2, Equation (7).  
 $P_1$  = " Induced " power loss }  
 $P_2$  = Profile drag power loss } (Lbs. ft. per second.)  
 $k_{P_1} = P_1/2\pi \rho n^3 D^5$  }  
 $k_{P_2} = P_2/2\pi \rho n^3 D^5$  } §2 (9) and (12); §3.2 (5) and (6).
-

1. *Introduction.*—The present report describes a rapid method of carrying out airscrew strip theory calculations by means of suitable charts. The method may be based either on the standard formulae of the “vortex theory” assuming an infinite number of blades (R. & M. 892<sup>1</sup>), or on the improved formulae described in R. & M. 1377<sup>2</sup> and R. & M. 1521<sup>3</sup> which include a correction for tip loss.

In carrying out a detailed strip theory calculation on the basis of either assumption by standard methods (as described, e.g., in R. & M. 892<sup>1</sup> or R. & M. 1674<sup>5</sup>) it is assumed that values of the lift and drag coefficients of the section, in two dimensional flow, are known, at a series of standard radii, as well as the chord and blade angle of the sections. It is then possible, for each standard radius and for *assumed values of the blade incidence*, to calculate values of  $J (= V/nD)$  and of thrust and torque grading, but it is necessary to cross plot in order to obtain values of thrust and torque grading for given  $J$  before drawing and integrating the thrust and torque grading curves.

The charts here described make it possible to determine thrust and torque grading directly for given values of  $J$  and so avoid not only the labour of computing the formulae but also the labour of cross plotting. The method is specially convenient when results are required for a single working condition only. There still remains, however, the labour of drawing the thrust and torque grading curves and integrating them graphically. The only way of obtaining further simplification is to confine the calculations to a single standard radius and (assuming the *shape* of the thrust grading curves, etc., to be the same for all cases) to use a constant integrating factor to determine the area. Considerable success has been attained with the application of this simplification to the airscrews tested in the recent research on high pitch models at the National Physical Laboratory<sup>4</sup> and the combination of this method with the graphical method is the principal subject of this report. The combination of the two reduces the labour of calculation to such an extent that the performance of a given airscrew at a single value of  $J$  can be obtained in a few minutes and its complete performance in considerably under an hour.

2. *Basis of Graphical Method.*—We proceed to describe the graphical method as applied to calculate the performance of a blade element at a given radius for a given value of  $J$ . The method has become possible as a result of neglecting the profile drag in calculating the interference velocity. It has been shown that this omission is fully justified at any rate so long as the blade section is operating below the stalling angle.<sup>5</sup> The formulae thus simplified are given in Ref. 3, p. 22, and in Ref. 5, §3.

For the purpose of computing the charts it is convenient to use a slightly modified set of formulae. These may be obtained most simply from the geometry of Fig. 1 together with the fundamental relation

$$w_1 = \frac{sk_L W}{2\kappa \sin \phi}, \quad \dots \dots \dots (1)$$

which is identical with Ref. 5, p. 4, equation (7). Here  $k_L$  is the lift coefficient of the blade section in two dimensional flow,  $s$  is the solidity ratio at radius  $r$  given by

$$s = \frac{Nc}{2\pi r},$$

(where  $N$  is the number of blades and  $c$  is the chord length of the section), and  $\kappa$  is the tip loss coefficient defined in Ref. 5, §2. The formulae may also be easily verified algebraically from those of Ref. 5.

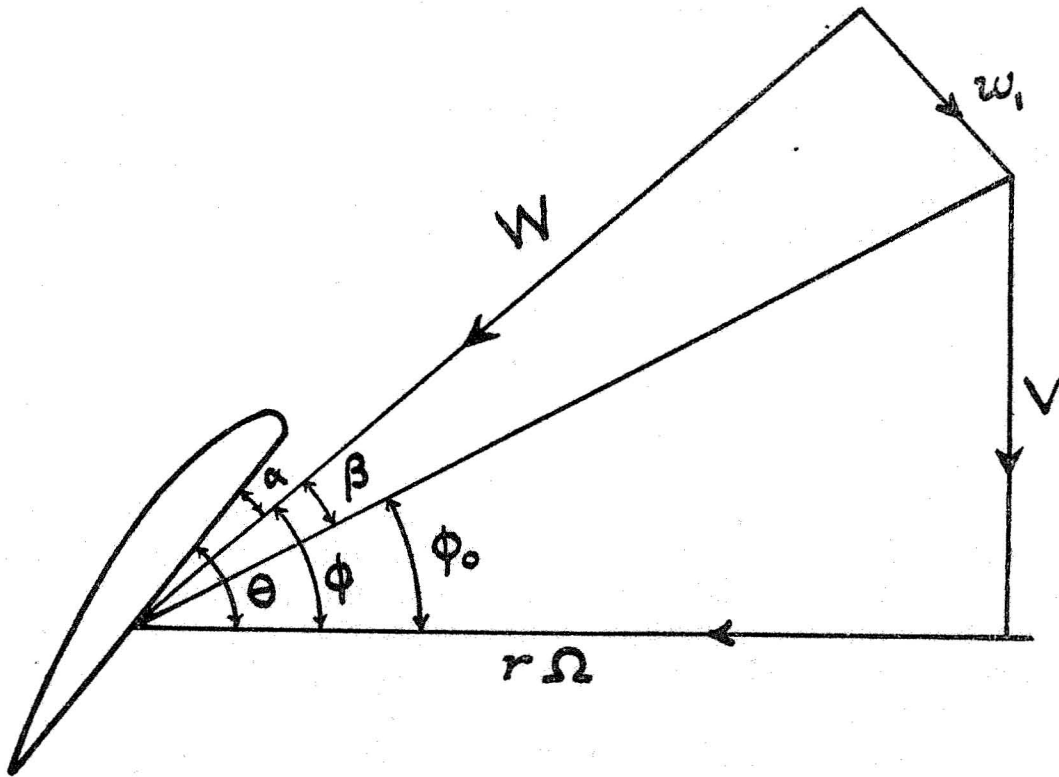


FIG. 1.

The figure is similar to Fig. 1 of Ref. 5 and represents the various velocity components in a plane at right angles to a blade at radius  $r$ .

In calculating the charts it is convenient to use  $J$  ( $\equiv \pi V/R\Omega$ ) and  $\beta$  (Fig. 1) as independent variables. Then  $\phi_0$  is given by the equation

$$\begin{aligned} \tan \phi_0 &= V/r\Omega \\ &= J/\pi x, \quad \dots \dots \dots (2) \end{aligned}$$

and  $\phi$  is given by

$$\phi = \phi_0 + \beta. \quad \dots \dots \dots (3)$$

From equation (1)

$$sk_L = 2\kappa \sin \phi \tan \beta , \quad \dots \quad \dots \quad (4)$$

since

$$w_1/W = \tan \beta ,$$

by the geometry of the figure. Equations (2), (3) and (4) determine  $sk_L$  as a function of  $J$  and  $\beta$ ; or  $J$  and  $\phi$  only (for given  $\kappa$ ) since  $\kappa$  is a known function of  $\phi$  and  $\kappa$  (for a given number of blades) by the Tables or Charts of Ref. 5 (Table 1 and Figs. 3, 4, 5 and 6). These equations do not involve  $s$  and  $k_L$  separately nor do they contain the blade angle  $\theta$  nor the incidence  $\alpha$ . It is therefore possible to construct chart 1 (Fig. 2)\* consisting of a set of curves of  $sk_L$  against  $\phi$  for a series of constant values of  $J$ .

The essential feature of the method is the use of this chart in conjunction with Chart 2 (Fig. 3) consisting of curves of  $sk_L$  against  $\alpha$  for a series of constant values of  $s$ , derived from the lift curve of the blade section in two dimensional flow. Chart 1 is superposed on Chart 2 (one of these two charts must be transparent), the scale of  $\phi$  in Chart 1 being equal but in the opposite sense to the scale of  $\alpha$  in Chart 2. The zero of  $\alpha$  on Chart 2 is adjusted to coincide with a value of  $\phi$  in Chart 1 equal to the known value of the blade angle  $\theta$  of the section. The value of  $\phi$  for any point on Chart 1 and the value of  $\alpha$  for the corresponding point on Chart 2, then satisfy the geometrical relation (Fig. 1).

$$\phi = \theta - \alpha . \quad \dots \quad \dots \quad \dots \quad (5)$$

Hence the point of intersection of the curve of Chart 1 for a given value of  $J$  with the curve of Chart 2 for a given value of  $s$  (corresponding to the chord length of the section) determines values of  $sk_L$  (and  $k_L$ ),  $\phi$  and  $\alpha$ , which are solutions of equations (2, 3, 4 and 5), for a given value of  $J$ ; from these the thrust and torque of the blade element can be determined when the blade angle  $\theta$ , the "solidity"  $s$  and the relation between  $k_L$  and  $\alpha$  are known. This result could not be obtained arithmetically for given  $J$  except by successive approximation. The dotted curve in Chart 1 shows the position of the curve of  $sk_L$  against  $\alpha$  of Chart 2, for  $s = 0.07$  with the zero adjusted for  $\theta = 24.45^\circ$  corresponding to an airscrew of  $P/D$  1.0. Its intersection with the curve for (e.g.)  $J = 0.8$ , gives:—

$$sk_L = 0.0225 , \quad \phi = 22.45^\circ , \quad \alpha = 2.00^\circ .$$

Now that  $\alpha$  (or  $sk_L$ ) is known it is a simple matter to determine the thrust coefficient of the blade element and the "induced power loss". These may be most conveniently obtained from Charts 3

\* Tables 1 and 2 contain data for constructing the charts (for radius  $\kappa = 0.7$  only); they should of course be drawn on a considerably larger scale.

and 4 (Figs. 4 and 5) consisting of curves of  $dk_T/d(x^2)$ , and  $\frac{1}{2}w_c$  respectively against  $sk_L$  for a series of constant values of  $J$ . These charts are computed from the following formulae derivable from the geometry of Fig. 1.

$$\begin{aligned} w_c &\equiv w_1 \sec \phi / R\Omega \quad (\text{definition}) \\ &= \frac{x \sin \beta}{\cos \phi_0 \cos \phi}, \quad \dots \quad \dots \quad \dots \quad \dots \quad (6) \end{aligned}$$

$$\begin{aligned} W_c &\equiv W/R\Omega \quad (\text{definition}) \\ &= x \cos \beta / \cos \phi_0 \quad \dots \quad \dots \quad \dots \quad \dots \quad (7) \end{aligned}$$

Neglecting the contribution of the profile drag to the thrust (which is justifiable below the stalling angle), the element of thrust on a blade element is given by

$$dT = \rho c dr \cdot W^2 k_L \cos \phi,$$

so that

$$\frac{1}{\rho(R\Omega)^2} \cdot \frac{1}{\pi} \cdot \frac{dT}{d(r^2)} = sk_L W_c^2 \cos \phi$$

and

$$\frac{dk_T}{d(x^2)} = \frac{\pi^3}{4} \cdot sk_L \cdot W_c^2 \cos \phi \quad \dots \quad \dots \quad \dots \quad (8)$$

Similarly the element of thrust power loss is (Ref. 5, §3 (11))

$$dP_1 = w_1 dT \sec \phi,$$

and its coefficient is given by

$$\frac{dk_{P_1}}{d(x^2)} = \frac{1}{2} w_c \frac{dk_T}{d(x^2)}, \quad \dots \quad \dots \quad \dots \quad \dots \quad (9)$$

derivable from Ref. 5, §3, (17) and (33).

It has been found convenient to use the chart of  $w_c$  against  $sk_L$  (Chart 4, Fig. 5) in combination with equation (9), rather than to construct a chart of  $dk_{P_1}/d(x^2)$ , because  $w_c$  (as well as  $dk_T/d(x^2)$ ) is nearly linear in  $sk_L$ .

In order to obtain the torque and efficiency from the equations

$$k_Q = (J k_T / 2\pi) + k_{P_1} + k_{P_2}, \quad \dots \quad \dots \quad (10)$$

$$1 - \eta = \frac{k_{P_1} + k_{P_2}}{k_Q}, \quad \dots \quad \dots \quad \dots \quad \dots \quad (11)$$

(Ref. 5, §3, (34) and (35)) it is necessary to obtain the coefficient of profile drag power loss at the blade element. This is given by the equation

$$dk_{P_2}/d(x^2) = (\pi^3/8) sk_D W_c^3, \quad \dots \quad \dots \quad \dots \quad (12)$$

derivable from Ref. 5, §3, (18) and (33). In equation (7)  $\beta$  is seldom greater than  $10^\circ$  and so  $W_c$  is practically a function of  $\phi_0$  or  $J$  only (for given  $x$ ). A table or curve of  $\frac{\pi^3}{8} W_c^3 \left( = \frac{1}{sk_D} \cdot \frac{dk_{P_2}}{d(x^6)} \right)$  as a function of  $J$  is therefore prepared by putting  $\beta = 6^\circ$  say, in equation (5) giving,  $\cos \beta = 0.995$ , (Fig. 6). A value of  $sk_D$  is determined from the profile drag coefficient of the blade section plotted against  $\alpha$  (Chart 6, Fig. 7). If desired a chart of  $dk_{P_2}/d(x^2)$  against  $sk_D$  for given  $J$  may be prepared, the curves being straight lines.

An essential feature of the method is that the 3 charts 1, 3 and 4 (with curve 5) are of universal application for a given radius and number of blades, being independent of blade section, chord and blade angle. Charts 2 and 6 on the other hand involve the lift and drag coefficients of the particular blade section, with a constant multiplier for blade width but are not affected by the blade angle or the particular value of  $J$ . The combined charts cover all values of  $\theta$  and  $s$  up to the limits of the scales of  $sk_L$  and  $\phi$ .

It is proposed to calculate sets of Charts 1, 3 and 4 over suitable ranges of  $sk_L$  for radii  $x = 0.3, 0.45, 0.6, 0.7, 0.8, 0.9$  and  $0.95$  and for 2, 3 and 4 bladed airscrews. The method will then determine  $dk_T/d(x^2)$ ,  $dk_{P_1}/d(x^2)$ ,  $dk_{P_2}/d(x^2)$  for a series of even values of  $J$  at all the standard radii, and it will then only be necessary to plot these three coefficients against  $x^2$  and integrate graphically in order to obtain  $k_T$  and  $k_{P_1} + k_{P_2}$ . (See Ref. 5, Figs. 10, 11 and 12.) The torque coefficient and efficiency are then given by equations (10) and (11).

The effect of compressibility could be included in calculations by this method provided that the values of  $k_L$  and  $k_D$  for the sections, considered as functions of the ratio of the velocity to the velocity of sound, were known. Conversely the method would be very convenient for analysing observations of the type made at the R.A.E. on high tip speed airscrews, Ref. 6.

Charts for use by the above method are being calculated at the time of writing but have not yet been used. The method has only been used in conjunction with the further simplification of making calculations at a single radius and using integrating factors. This method will be described in the next section, being to some extent independent of the graphical method and having been used first in point of time.

3. *Simplified Method of Calculation.*—In order to save part of the labour of making detailed strip theory calculations, attempts have often been made in the past to use calculations at a single standard radius, and to determine the thrust and torque by means of integrating factors. It seemed worth while to attempt this method on the basis of the assumptions of Refs. 2 and 3. The use of charts of the type already described is specially convenient when



working at a single standard radius. The method has the additional advantage that it can be used either *directly*, to calculate the thrust and torque of the airscrew from the lift and drag curves of the standard section, or *inversely* to deduce lift and drag curves of the standard section from the thrust and torque of the airscrew. The thrust and torque of a typical airscrew might be calculated by the detailed strip theory set forth in §2 and afterwards the inverse method for a standard section employed to deduce lift and drag curves.

It is evident that the success of the present method does not require that the fictitious lift and drag deduced in this way should agree closely with the true lift and drag of the section at the standard radius; it is sufficient if the same lift and drag curves are deduced from an analysis of screws of widely different pitch, solidity and plan form having the same blade section at the standard radius. As a first test of this method it is therefore convenient to use it to analyse the experiments on a family of model airscrews described in Ref. 4.

3.2. *Inverse method.*—When thrust grading curves are plotted on a basis of radius squared as in Ref. 5, Fig. 10, in accordance with §2 (8), the curve approximates in form to a semi-circle or semi-ellipse for which the area would have the value

$$\frac{\pi}{4} \times \text{mid ordinate.}$$

The mid ordinate corresponds to  $x^2 = 0.5$  or  $x = 0.707$  and the value  $x = 0.7$  has been chosen for convenience. The procedure is otherwise precisely similar to that used in detailed strip theory calculations except that the formulae

$$k_T = \int \{dk_T/d(x^2)\} d(x^2) \quad \dots \quad (1)$$

$$k_{P_1} = \int \{dk_{P_1}/d(x^2)\} d(x^2) \quad \dots \quad (2)$$

$$k_{P_2} = \int \{dk_{P_2}/d(x^2)\} d(x^2) \quad \dots \quad (3)$$

are replaced by

$$\begin{aligned} k_T &= \frac{1}{4}\pi dk_T/d(x^2) \\ &= (\pi^4/16) sk_L W_c^2 \cos \phi, \quad \dots \quad (4) \end{aligned}$$

$$\begin{aligned} k_{P_1} &= \frac{1}{4}\pi dk_{P_1}/d(x^2) \\ &= \frac{1}{2}w_c k_T, \quad \dots \quad (5) \end{aligned}$$

$$\begin{aligned} k_{P_2} &= \frac{1}{4}\pi dk_{P_2}/d(x^2) \\ &= (\pi^4/32) sk_D W_c^3. \quad \dots \quad (6) \end{aligned}$$

The chart of  $sk_L$  against  $\phi$  for given  $J$  (Chart 1, Fig. 2) is constructed for radius 0.7, as well as the chart of  $w_c$  against  $sk_L$  (Chart 4); the chart of  $dk_T/d(x^2)$  and curve of  $(1/sk_D) \times (dk_{P_2}/d(x^2))$ , (Charts 3 and 5) are replaced by a chart of  $k_T$  against  $sk_L$  and a curve of  $k_{P_2}/sk_D$  against  $J$  according to equations (4) and (6), (Figs. 4 and 6).

The inverse of the method described in §2 is then employed to deduce curves of  $k_L$  and  $k_D$  against  $\alpha$  from observed performance curves of an airscrew in the form of curves of  $k_T$  and  $k_Q$  against  $J$ . First read off  $sk_L$  from Fig. 4 for given  $J$  and  $k_T$ . Next read off  $\phi$  from Fig. 2 for given  $J$  and  $sk_L$  and deduce  $\alpha$  from § 2(5). To obtain  $k_D$  determine  $w_c$  from Chart 4, Fig. 5, from the observed value of  $J$  and from the deduced value of  $sk_L$ . Then obtain  $k_{P_2}$  from the relation

$$k_{P_2} = k_Q - J k_T / 2\pi - \frac{1}{2} w_c k_T ,$$

using the observed values of  $k_T$ ,  $k_Q$  and  $J$ , and deduce  $sk_D$  from the curve of  $k_{P_2}/sk_D$  against  $J$  in Fig. 5.\*

The observed thrust and torque coefficients of the main series of two and four bladed model airscrews of varying pitch<sup>4</sup> have been analysed in this way, and the values of  $k_L$  and  $k_D$  deduced from them are plotted in Figs. 8 and 9 for the two bladers. The results for the four bladers are similar, and the smoothed values for two and four blades as well as the mean of the values for two and four blades are recorded in Table 3.

The extent of the variation of the  $k_L$  and  $k_D$  curves with pitch for two bladed airscrews is shown in Figs. 8 and 9 and the results for two bladed and four bladed airscrews were found to be in reasonably good agreement with each other. For a range of pitch from 0.3 to 1.5 the agreement on  $k_L$  below the stall is good enough for practical purposes; at still higher pitch values there is a small but definite variation with pitch.

The  $k_D$  points appear to be more scattered than the  $k_L$  points but for the higher pitched screws the contribution of the drag to the torque is small; in the extreme case of the lowest  $k_D$  ( $P/D$  2.5) shown in Fig. 9, the drag contributes only  $3\frac{1}{2}$  per cent. to the torque observation from which it was deduced. Thus for a screw of this pitch the extreme variations in Fig. 9 would correspond to variations of only about 1 per cent. on torque. It has been verified by comparison with direct strip theory calculations that the tendency for the  $k_L$  values of the highest pitch airscrews (Fig. 8) to depart from the mean curve is due almost entirely to the assumption of a constant integrating factor, since the detailed strip theory results (Ref. 5) are in good agreement with experiment.

3.3. *The Direct Method.*—The direct application of the graphical method at a single standard radius now requires little further explanation.† The method described in Section 2 is followed in detail except that the chart of  $dk_T/d(x^2)$  against  $sk_L$  and the curve of  $(1/sk_D) \times dk_{P_2}/d(x^2)$  against  $J$  (Figs. 4 and 6) are replaced by a chart of  $k_T$  against  $sk_L$  and a curve of  $k_{P_2}/sk_D$  against  $J$  respectively according to equations (4) and (6) of §3.2.

\* A detailed example is given in Appendix A.1.

† A detail calculation is given in the Appendix A.2.

The most useful course for the practical designer of airscrews who uses a definite set of blade sections will be to compute the thrust and torque of a typical screw (of P/D 1.5 say) by detailed strip theory below the stall (assuming that the lift and drag of the sections is known), and then to employ the *inverse* method of §3.2 to deduce standard  $k_L$  and  $k_D$  curves which could be used in conjunction with the *direct* method to calculate the performance of screws over a wide range of pitch and solidity. In the absence of data of this kind (and in any case above the stall) it is suggested that the values of  $k_L$  and  $k_D$ , given in Table 3, which were deduced from the model airscrew experiments of Ref. 4, should be used for this purpose.

In order to secure the greatest possible economy of time in calculating  $k_Q$  it would be desirable to construct a chart of:—

$$(J k_T/2\pi + \frac{1}{2}w_c k_T)$$

against  $sk_L$ . Then  $k_{P_2}$  is deduced from the curve of  $k_{P_2}/sk_D$  against J, and  $k_Q$  is given by

$$k_Q = (J k_T/2\pi + \frac{1}{2}w_c k_T) + k_{P_2} \quad \dots \quad (1)$$

It is reasonable to assume that the results are valid over a large range of values of  $s$  (*solidity ratio*) and for a complete range of *angles of pitch* (to the degree of accuracy indicated by Figs. 8 and 9). A change of *blade twist* or of *plan form* might affect the lift and drag curves obtained from analysis of airscrew performance in so far as these curves differ from the actual lift and drag curves of the section at radius 0.7 (Fig. 10); the required alteration might be calculated on the basis of detailed strip theory, or a model test of a typical airscrew. The  $k_L$  and  $k_D$  values of Table 3 (mean of 2 and 4 blades) are compared in Fig. 10 with the measured lift and drag curves of the section at radius 0.7 (deduced by interpolation from Table 3 of R. & M. 892<sup>1</sup>). The lift curves are in good agreement near zero lift but there is an appreciable difference at high lifts and a similar disagreement on drag in the high lift region. The values of maximum lift and minimum drag are however in reasonably good agreement. The effect of change of *blade section* should be allowed for by alteration of the lift and drag curves either directly on the basis of a test of the aerofoil section at a radius 0.7 or of a calculation by the theory of thin aerofoils (Fig. 10) for the lift, and by estimation for the drag.

4. *Tables for constructing charts.*—Tables 1 and 2 give values of the quantities  $\phi$ ,  $sk_L$ ,  $w_c$ ,  $k_T$ , as functions of J and  $\beta$ , and of  $k_{P_2}/sk_D$ , as a function of J, (for  $\beta = 6^\circ$  only) for radius  $x = 0.7$ . These quantities are directly calculated\* by means of formulae (2), (3), (4), (6) and (7) of §2 and (4) and (6) of §3.2, combined with values of  $\alpha$  derived from Ref. 5, Figs. 3, 4, 5 and 6. Of these quantities,  $\phi$ ,  $w_c$ , and  $k_{P_2}$  are independent of number of blades for given  $\beta$  so that

\* It is unnecessary to calculate every entry in the table directly, as intermediate values may be filled in by plotting the figures in any column against J.

only  $sk_L$  and  $k_T$  have to be repeated when  $N$  varies. Results for 2, 3 and 4 blades are given in Table 1 while values of  $sk_L$  and  $k_T$  for 6 blades and infinity blades are given separately in Table 2 as they are less often required. Charts 1, 3, 4 and 5 can be constructed by direct plotting from these tables, and it seemed preferable to publish the tables rather than to attempt to reproduce the charts themselves on a sufficiently large scale.

5. *Further Simplification for the Torque.*—In so far as the contribution of the drag to the torque is fairly small below the stall, especially for high pitch airscrews, it might be worth while to assume the drag coefficient to be independent of incidence; on this assumption  $k_Q$  is a function of  $sk_L$ ,  $J$  and  $s$  only, which varies only slowly with  $s$  so that a limited number of charts for different values of  $s$  would determine values of  $k_Q$  directly without the need of using Figs. 6 and 7 and equation (10) of §2 or (1) of §3.3. This further simplification suggests the possibility of using the method to analyse full scale airscrew data in which the forward speed, rotational speed and engine power only are known. The best way to do this would be to estimate the profile drag power from curves such as Figs. 2–7 already available, and then to use the observed torque power less profile drag power, to calculate a point on a curve of  $sk_L$  against  $\alpha$ , precisely as was done in §3.2 on the basis of observed thrust coefficient.

6. *Stalled Range.*—The simplified method of §3 has been applied successfully to a stalled airscrew, with the single modification that it has been necessary to replace equation §2 (8) or §3.2 (4) by the more exact equations

$$\left. \begin{aligned} dk_T/d(x^2) &= (\pi^3/4) s W_c^2 (k_L \cos \phi - k_D \sin \phi) \\ k_T &= (\pi^4/16) s W_c^2 (k_L \cos \phi - k_D \sin \phi) \end{aligned} \right\} \dots (1)$$

(Ref. 5, p. 8, equation 24). According to this equation the method of analysis described in §3.2 determines the value of

$$sk_{L_0} = sk_L - sk_D \tan \phi \quad (\text{definition of } k_{L_0}) \dots (2)$$

and also values of  $sk_D$  and of  $\phi$ , so that the true value of  $sk_L$  can at once be calculated. In Fig. 8, all points for which  $\alpha$  is greater than  $10^\circ$  include this correction and it is evident that results above the stall deduced from airscrews of varying pitch are reasonably consistent. In the direct application of the method the value of  $\phi$  is at first unknown, and it would be necessary to proceed by successive approximation. The method is described in detail in Appendix A.3 which shows that the additional labour required is quite small.

It is important to emphasize that beyond the stall the results of detailed strip theory calculations based on aerofoil data at present available have been found to be unreliable, and that it is essential to use the lift and drag coefficients for the standard sections (such as those of Table 3) derived from tests of actual airscrews.

7. *Conclusions.*—The simplifications of strip theory calculations described in the present report have arisen naturally from two modifications of the standard formulae as described in R. & M. 1377<sup>2</sup>.

(1) The omission of the profile drag coefficient in calculating the interference velocity; this made the graphical method possible.

(2) The use of thrust grading curves plotted on a base of the square of the radius instead of the first power. This suggested the possibility of obtaining reasonably accurate results by making calculations at a radius 0·7 and using integrating factors.

A very rapid method of computing airscrew performance has been developed which gives good accuracy up to  $P/D$  1·0 or 1·5 and fair accuracy up to  $P/D$  2·5.

It would be possible to include the effect of compressibility of the air in calculations by the approximate method of §3 but the accuracy obtainable is doubtful because the effect falls off rapidly on proceeding inwards from the blade tip. The possible accuracy could be determined by comparison with detailed strip theory calculations in which the effect of compressibility was included; for this purpose the graphical method as described in §2 would be convenient.



## APPENDIX

A.1. *Detailed calculation by inverse method (§3.2).*—Analysis of observed performance on a model airscrew. Airscrew 2 blades, standard section and width, P/D 1.5 (normal blade angles). Observed data (from Ref. 4, Table 5, p. 18).

J	0.19	0.30	0.40	0.60	0.80	1.00	1.20	1.40	1.60	1.76
$k_T$	0.1310	0.1330	0.1340	0.1330	0.1265	0.1085	0.0855	0.0590	0.0285	0
$k_Q$	0.0244	0.0227	0.0218	0.0214	0.0220	0.0213 <sub>5</sub>	0.0189 <sub>5</sub>	0.0149 <sub>5</sub>	0.0091 <sub>5</sub>	0.0030

Blade angle  $\theta = 34^\circ 19'$ ,  $s = 0.0705$ , at  $x = 0.7$ .

Details of calculation for  $J = 0.30$ .

From Chart 3, for  $k_T = 0.1310$ ,  $J = 0.30$ , read off  $sk_{L_0} = 0.0457$ .

From Chart 1, for  $sk_{L_0} = 0.0457$ ,  $J = 0.30$ , read off  $\phi = 14^\circ 6'$ .

Then  $\alpha = \theta - \phi = 20^\circ 13'$ .

From observed values, work out  $k_Q - \frac{Jk_T}{2\pi}$  (total power loss) = 0.0163<sub>5</sub>.

From Chart 4, for  $sk_{L_0} = 0.0457$ ,  $J = 0.30$ , read off  $w_c = 0.0799$  and calculate  $k_{P_1} = \frac{1}{2}w_c k_T = 0.0053$ .

Then  $k_{P_2} = k_Q - Jk_T/2\pi - k_{P_1} = 0.0110_5$ .

From curve of Chart 5,  $k_{P_2}/sk_D = 1.054$ , so that  $sk_D = 0.01048$ ,  $sk_D \tan \phi = 0.00263$ ,  $sk_L$  (accepted value) =  $sk_{L_0} + sk_D \tan \phi^* = 0.0483$ .

Hence for  $\alpha = 20^\circ 13'$ ,  $k_L = 0.686$ ,  $k_D = 0.149$ .

The complete results are given in the following Table and plotted in Figs. 8 and 9.

J =	0.19	0.30	0.40	0.60	0.80	1.00	1.20	1.40	1.60	1.76
$\alpha =$	22° 14'	20° 13'	17° 56'	14° 4'	9° 59'	6° 20'	3° 9'	0° 7'	-2° 29'	-4° 27'
$k_L =$	0.687	0.686	0.683	0.651	0.587	0.486	0.369	0.242	0.111	0
$k_D =$	0.201	0.149	0.109	0.051	0.022	0.011 <sub>5</sub>	0.007	0.007 <sub>5</sub>	0.012	0.020

A.2. *Detailed calculation by direct method (§3.3) (below the stall).*—Calculation of performance of an airscrew having 3 blades, solidity 0.100, P/D 1.1. The data used are the values of  $k_L$  and  $k_D$  given in Table 3 derived from analysis of the model tests of Ref. 4. Results therefore apply strictly to a screw having the same section and plan form as those models.

Blade angle at 0.7 is  $0.7 \pi \tan \theta = 1.1$ ,  $\theta = 26.6^\circ$ .

Details of the calculation for  $J = 0.8$ . As explained in Section 3.3 the transparent Chart 1 (for 3 blades  $x = 0.7$ ) of  $sk_L$  plotted against  $\phi$  is superposed on Chart 2 (or the single curve of  $sk_L$  against  $\alpha$  for  $s = 0.1$ ) so that the axis of  $\phi$  in Chart 1 coincides with the axis of  $\alpha$  of Chart 2 while the zero of the scale of Chart 2 coincides with the point  $\phi = 26.6^\circ$ , equal to the known value of  $\theta$ . Then the value of  $sk_L$  for any value of  $J$  may be read off without shifting the charts. For  $J = 0.8$  the point of intersection gives  $sk_L = 0.0370$ ,  $\phi = 23.4^\circ$ ,  $\alpha = 3.2^\circ$ ; these values satisfy the relation  $\phi = \theta - \alpha$ . Next the value of  $k_T = 0.1115$  is read from Chart 3 for  $J = 0.8$ ,  $sk_L = 0.0370$ .

\* This term may be omitted below the stall, i.e., for values of  $\alpha$  less than  $10^\circ$ .

From Chart 4 for  $sk_L = 0.0370$ ,  $J = 0.8$ , read of  $f_{\frac{1}{2}}w_c = 0.0232$  and so  $k_{P_1} = \frac{1}{2}w_c k_T = 0.0026$ .

From Table 1 or Chart 5, for  $J = 0.8$ ,  $k_{P_2}/sk_D = 1.240$ .

From Chart 6 for  $\alpha = 3.2^\circ$ ,  $sk_D = 0.0009$  and so  $k_{P_2} = 0.0011$ .

Finally  $k_Q = J k_T/2\pi + k_{P_1} + k_{P_2} = 0.0146 + 0.0026 + 0.0011 = 0.0183$ .

The calculation may be slightly simplified by using a chart of  $(J k_T/2\pi + k_{P_1})$  against  $sk_L$  in place of Chart 4 ( $w_c$  against  $sk_L$ ).

Results for the complete working range are given in the following Table.

J	1.3	1.2	1.1	1.0	0.8	0.6	0.4	0.2	0
$sk_L$	0.0033	0.0105	0.0178	0.0241	0.0370	0.0490	0.0587	0.0653	0.0665
$\phi$	30.9	29.5	28.0	26.5	23.4	19.9	16.6	13.6	10.6
$\alpha$	-4.3	-2.9	-1.4	-0.1	3.2	6.7	10.0	13.0	16.0
$sk_D$	0.0020	0.0013	0.0010	0.0009	0.0009	0.0015	0.0025	0.0045	0.0085
$k_T$	0.0115	0.0340	0.0590	0.0780	0.1115	0.1455	0.1705	0.1872	0.1875
$k_Q$	0.0056	0.0087	0.0124	0.0148	0.0183	0.0202	0.0205	0.0204	0.0209

For  $J = 0.2$  and 0 the calculations have been repeated by the method of the next section A.3 appropriate to the range beyond the stall; the modified results are

J	$sk_L$	$sk_{L_0}$	$\phi$	$\alpha$	$sk_D$	$k_T$	$k_Q$
0.2	0.0654	0.0643	13.4°	13.2°	0.0048	0.1840	0.0205
0	0.0666	0.0650	10.4°	16.2°	0.0088	0.1845	0.0209

The effect of the correction for stalling is evidently small for a screw of this pitch value.

*A.3. Direct calculation above the stall.*—Owing to the necessity of taking account of the term  $sk_D \tan \phi$  in §6 (2) it is necessary to proceed by successive approximation, but the convergence of the process will be found to be so rapid that very little extra labour is required.

Beyond the stall,  $sk_L$  is a function of  $\alpha$  (Chart 2) which varies slowly with  $\alpha$  while  $sk_{L_0}$  is a function of  $\phi$  (Chart 1) such that  $\phi$  varies slowly with  $sk_{L_0}$ ;  $sk_L$  and  $sk_{L_0}$  satisfy the relation §6 (2):—

$$sk_{L_0} = sk_L - sk_D \tan \phi$$

These considerations suggest the process illustrated by the following example. The essential point is that (after the first step) Chart 1 is used to deduce  $\phi$  from  $sk_{L_0}$  and Chart 2 is used to deduce  $sk_L$  from  $\alpha$  throughout the process.

Airscrew:—standard 2 blader, P/D 1.8;  $\theta = 39.33^\circ$  and  $s = 0.0705$  at  $x = 0.7$ . The mean values of  $k_L$  and  $k_D$  from Table 3 are used in constructing Charts 2 and 6. The numerical values refer to  $J = 0.3$ .

*First Approximation*, determine  $\phi$  ( $14.4^\circ$ ),  $\alpha$  ( $24.93^\circ$ ) and  $sk_L$  ( $0.0487$ ), (not  $sk_{L_0}$ ) by the use of Charts 1 and 2 exactly as described in A.2; deduce  $sk_D$  ( $0.0173$ ) from  $\alpha$  by Chart 6 and obtain  $sk_D \tan \phi$  ( $0.0044$ ). Then:—

*Second Approximation*

$$sk_{L_0} = sk_L - sk_D \tan \phi = 0.0443.$$

Deduce  $\phi$  ( $14.0^\circ$ ) from  $sk_{L_0}$  using Chart 1.

Deduce  $\alpha$  ( $25.33^\circ$ ) from the relation  $\alpha = \theta - \phi$ .

Deduce  $sk_D$  ( $0.0179$ ) from  $\alpha$  using Chart 6.

$$sk_D \tan \phi = 0.0044_5$$

$sk_L$  ( $0.0485$ ) from  $\alpha$  using Chart 2.

*Third approximation.*

$$sk_{L_0} = sk_L - sk_D \tan \phi = 0.0440_5.$$

A repetition of the process then gives  $\phi = 13.95^\circ$ ,  $\alpha = 25.38^\circ$ ,  $sk_D = 0.0179_5$ ,  $sk_L \tan \phi = 0.00445$ ,  $sk_L = 0.0485$ .

The subsequent operations are precisely the same as in A.2. using  $sk_{L_0}$  and  $sk_D$ .

It is evident that the values given by the second approximation ( $sk_{L_0} = 0.0440_5$ ),  $sk_D = 0.0179$  are accurate enough for all purposes, while for most purposes the first approximation to  $sk_{L_0}$  ( $0.0443$ ) is sufficiently accurate. The complete results of the calculation for a series of values of J are given in the following Table.

J	0.3	0.4	0.6	0.8	1.0
$\phi$	$14.0^\circ$	$16.0^\circ$	$20.2^\circ$	$24.7^\circ$	$28.6^\circ$
$\alpha$	$25.33^\circ$	$23.33^\circ$	$19.13^\circ$	$14.63^\circ$	$10.73^\circ$
$sk_{L_0}$	0.0440	0.0438	0.0440	0.0444	0.0415
$sk_L$	0.0485	0.0481	0.0475	0.0465	0.0426
$sk_D$	0.0179	0.0151	0.0096	0.0046	0.0021
$k_T$	0.1280	0.1282	0.1313	0.1355	0.1305
$k_Q$	0.0318	0.0290	0.0279	0.0274	0.0280

f

g  
e  
oh  
,.e.  
ce05  
n-



TABLE I

Table of values of  $\phi$  and  $w_c$  for given values of  $J$  and  $\beta$  for  $\alpha = 0.7$  and any number of blades. Also of  $(k_{P_2}/sk_D)$  for  $\beta = 6^\circ$ ; also of  $sk_L$  and  $k_T$  for 2, 3 and 4 blades.

$\beta^\circ$	$0^\circ$	$(6^\circ)$	$2^\circ$							
No. of blades			2 Blades		3 Blades		4 Blades			
J	$\phi_0$	$\frac{k_{P_2}}{sk_D}$	$\phi$	$w_c$	$sk_L$	$k_T$	$sk_L$	$k_T$	$sk_L$	$k_T$
0	0	1.026	$2^\circ 0'$	0.0244	0.0024	0.0071	0.0024	0.0071	0.0024	0.0071
0.05	$1^\circ 18'$		$3^\circ 18'$	0.0245	0.0041	0.0121	0.0041	0.0121	0.0041	0.0121
0.1	$2^\circ 36'$	1.030	$4^\circ 36'$	0.0245	0.0056	0.0168	0.0056	0.0168	0.0056	0.0168
0.15	$3^\circ 54'$		$5^\circ 54'$	0.0246	0.0071	0.0214	0.0071	0.0214	0.0071	0.0214
0.2	$5^\circ 12'$	1.042	$7^\circ 12'$	0.0247	0.0085	0.0253	0.0086	0.0257	0.0088	0.0262
0.25	$6^\circ 29'$		$8^\circ 29'$	0.0249	0.0098	0.0293	0.0101	0.0340	0.0104	0.0350
0.3	$7^\circ 46'$	1.054	$9^\circ 46'$	0.0250	0.0110	0.0330	0.0115	0.0340	0.0116	0.0350
0.35	$9^\circ 3'$		$11^\circ 3'$	0.0252	0.0121	0.0365	0.0129	0.0340	0.0132	0.0350
0.4	$10^\circ 18'$	1.074	$12^\circ 18'$	0.0254	0.0131	0.0396	0.0142	0.0429	0.0149	0.0443
0.45	$11^\circ 34'$		$13^\circ 34'$	0.0257	0.0140	0.0426	0.0155	0.0508	0.0159	0.0530
0.5	$12^\circ 48'$	1.106	$14^\circ 48'$	0.0259	0.0148	0.0452	0.0167	0.0508	0.0173	0.0530
0.55	$14^\circ 3'$		$16^\circ 3'$	0.0262	0.0155	0.0476	0.0177	0.0508	0.0184	0.0530
0.6	$15^\circ 15'$	1.148	$17^\circ 15'$	0.0265	0.0161	0.0497	0.0187	0.0576	0.0196	0.0604
0.65	$16^\circ 27'$		$18^\circ 27'$	0.0269	0.0168	0.0520	0.0196	0.0637	0.0207	0.0677
0.7	$17^\circ 39'$	1.190	$19^\circ 39'$	0.0272	0.0173	0.0540	0.0204	0.0637	0.0216	0.0677
0.75	$18^\circ 49'$		$20^\circ 49'$	0.0276	0.0177	0.0566	0.0211	0.0637	0.0226	0.0677

0.7 0.75	17° 39' 18° 49'	1.150	18° 20' 19° 49'	0.0276	0.0177	0.0572	0.0217	0.0687	0.0234	0.0742
0.8	19° 59'	1.240	21° 59'	0.0280	0.0181	0.0572	0.0217	0.0687	0.0234	0.0742
0.85	21° 7'		23° 7'	0.0285	0.0184	0.0588	0.0223	0.0732	0.0243	0.0809
0.9	22° 15'	1.294	24° 15'	0.0290	0.0187	0.0603	0.0229		0.0251	
0.95	23° 20'		25° 20'	0.0294	0.0190	0.0614	0.0235		0.0259	
1.0	24° 27'	1.362	26° 27'	0.0300	0.0191	0.0623	0.0239	0.0771	0.0265	0.0867
1.1	26° 34'	1.438	28° 34'	0.0311	0.0194	0.0635	0.0247	0.0807	0.0277	0.0909
1.2	28° 37'	1.522	30° 37'	0.0323	0.0199	0.0655	0.0254	0.0843	0.0287	0.0955 <sub>5</sub>
1.3	30° 36'	1.614	32° 36'	0.0337	0.0200	0.0677	0.0261	0.0879	0.0295	0.0997
1.4	32° 29'	1.710	34° 29'	0.0351	0.0202	0.0696	0.0265	0.0913	0.0301	0.1041
1.5	34° 18'	1.820	36° 18'	0.0367	0.0205	0.0720	0.0270	0.0946	0.0308	0.1086 <sub>5</sub>
1.6	36° 3'	1.936	38° 3'	0.0384	0.0207	0.0744	0.0274	0.0982	0.0314	0.1130
1.7	37° 42'	2.062	39° 42'	0.0401	0.0210	0.0768	0.0278	0.1017	0.0319	0.1172
1.8	39° 19'	2.210	41° 19'	0.0420	0.0212	0.0791	0.0280	0.1047	0.0324	0.1214
1.9	40° 50'	2.364	42° 50'	0.0440	0.0213	0.0811	0.0283	0.1078	0.0327	0.1250
2.0	42° 17'	2.536	44° 17'	0.0461	0.0215	0.0838	0.0285	0.1113	0.0331	0.1296
2.1	43° 41'	2.724	45° 41'	0.0484	0.0216	0.0858	0.0288	0.1143	0.0335	0.1333
2.2	45° 0'	2.910	47° 0'	0.0507	0.0217	0.0882	0.0290	0.1176	0.0337	0.1374
2.3	46° 17'	3.108	48° 17'	0.0531	0.0219	0.0906	0.0291	0.1206	0.0340	0.1411
2.4	47° 31'	3.328	49° 31'	0.0557	0.0220	0.0930	0.0293	0.1238	0.0343	0.1452
2.5	48° 40'	3.566	50° 40'	0.0584	0.0221	0.0954	0.0294	0.1271	0.0345	0.1492
2.6	49° 46'	3.826	51° 46'	0.0611	0.0221	0.0975	0.0296	0.1301	0.0347	0.1539
2.7	50° 51'	4.094	52° 51'	0.0641	0.0222	0.1001	0.0297	0.1333	0.0349	0.1575
2.8	51° 50'	4.368	53° 50'	0.0670	0.0222	0.1015	0.0298	0.1363	0.0350	0.1608
2.9	52° 49'	4.662	54° 49'	0.0705	0.0223	0.1039	0.0299	0.1394	0.0352	0.1646
3.0	53° 44'	4.964	55° 44'	0.0734	0.0223	0.1064	0.0299	0.1428	0.0354	0.1693

TABLE 1—continued

$\beta = 4^\circ$

J	$\phi$	$w_c$	2 Blades		3 Blades		4 Blades	
			$sk_L$	$k_T$	$sk_L$	$k_T$	$sk_L$	$k_T$
0	4°	0.0490	0.0096	0.0283	0.0096	0.0283	0.0096	0.0283
0.05	5° 18'	0.0491	0.0129	0.0381	0.0129	0.0463	0.0129	0.0465
0.1	6° 36'	0.0492	0.0157	0.0463	0.0157	0.0545	0.0157	0.0522
0.15	7° 54'	0.0494	0.0185	0.0545	0.0189	0.0640	0.0190	0.0652
0.2	9° 12'	0.0497	0.0210	0.0619	0.0217		0.0221	
0.25	10° 29'	0.0500	0.0233	0.0689	0.0246		0.0249	
0.3	11° 46'	0.0504	0.0254	0.0752	0.0274	0.0809	0.0280	0.0830
0.35	13° 3'	0.0508	0.0274	0.0810	0.0298	0.0955	0.0310	0.0989
0.4	14° 18'	0.0512	0.0290	0.0858	0.0323		0.0333	
0.45	15° 34'	0.0518	0.0305	0.0907	0.0346		0.0360	
0.5	16° 48'	0.0523	0.0319	0.0951	0.0368	0.1101	0.0384	0.1151
0.55	18° 3'	0.0530	0.0330	0.0986	0.0387	0.1210	0.0407	0.1283
0.6	19° 15'	0.0536	0.0342	0.1023	0.0403		0.0427	
0.65	20° 27'	0.0544	0.0351	0.1060	0.0418	0.1309	0.0446	0.1400
0.7	21° 39'	0.0552	0.0361	0.1093	0.0432		0.0461	
0.75	22° 49'	0.0560	0.0368	0.1120	0.0444	0.1397	0.0482	0.1533
0.8	23° 59'	0.0569	0.0374	0.1145	0.0456		0.0499	
0.85	25° 7'	0.0579	0.0378	0.1163	0.0468	0.1490	0.0514	0.1638
0.9	26° 15'	0.0589	0.0382	0.1184	0.0477		0.0528	

18



TABLE 1—continued

$\beta = 6^\circ$

J	$\phi$	$w_c$	2 Blades		3 Blades		4 Blades	
			$sk_L$	$k_T$	$sk_L$	$k_T$	$sk_L$	$k_T$
0	6°	0.0736	0.0216	0.0638	0.0217	0.0638	0.0217	0.0638
0.05	7° 18'	0.0738	0.0258	0.0753	0.0263	0.0753	0.0268	0.0753
0.1	8° 36'	0.0741	0.0299	0.0872	0.0309	0.0872	0.0311	0.0872
0.15	9° 54'	0.0744	0.0333	0.0969	0.0341	0.0969	0.0348	0.0969
0.2	11° 12'	0.0749	0.0368	0.1071	0.0392	0.1071	0.0400	0.1071
0.25	12° 29'	0.0754	0.0399	0.1162	0.0432	0.1162	0.0445	0.1162
0.3	13° 46'	0.0760	0.0426	0.1241	0.0473	0.1241	0.0486	0.1241
0.35	15° 3'	0.0767	0.0451	0.1300	0.0508	0.1300	0.0525	0.1300
0.4	16° 18'	0.0775	0.0471	0.1375	0.0541	0.1375	0.0563	0.1375
0.45	17° 34'	0.0783	0.0491	0.1438	0.0572	0.1438	0.0600	0.1438
0.5	18° 48'	0.0793	0.0507	0.1485	0.0597	0.1485	0.0634	0.1485
0.55	20° 3'	0.0803	0.0523	0.1537	0.0622	0.1537	0.0659	0.1537
0.6	21° 15'	0.0814	0.0538	0.1582	0.0643	0.1582	0.0691	0.1582
0.65	22° 27'	0.0825	0.0549	0.1623	0.0663	0.1623	0.0717	0.1623
0.7	23° 39'	0.0838	0.0559	0.1660	0.0681	0.1660	0.0745	0.1660
0.75	24° 49'	0.0852	0.0566	0.1690	0.0699	0.1690	0.0765	0.1690
0.8	25° 59'	0.0866	0.0575	0.1722	0.0714	0.1722	0.0789	0.1722
0.85	27° 7'	0.0871	0.0580	0.1743	0.0729	0.1743	0.0811	0.1743
0.9	28° 15'	0.0897	0.0584	0.1766	0.0741	0.1766	0.0827	0.1766

0.95

29° 20'

0.95	29° 20'	0.0915	0.0589	0.1791	0.0752	0.2343	0.0845	0.2649
1.0	30° 27'	0.0932	0.0594	0.1821	0.0765	0.2433	0.0862	0.2780
1.1	32° 34'	0.0970	0.0602	0.1863	0.0785	0.2512	0.0894	0.2890
1.2	34° 37'	0.1013	0.0611	0.1917	0.0800	0.2598	0.0911	0.3000
1.3	36° 36'	0.1059	0.0618	0.1972	0.0814		0.0931	
1.4	38° 29'	0.1108	0.0627	0.2027	0.0828	0.2677	0.0948	0.3106
1.5	40° 18'	0.1161	0.0633	0.2082	0.0838	0.2767	0.0966	0.320
1.6	42° 3'	0.1218	0.0639	0.2136	0.0848	0.2842	0.0981	0.331
1.7	43° 42'	0.1279	0.0645	0.2193	0.0856	0.2918	0.0994	0.341
1.8	45° 19'	0.1345	0.0651	0.2252	0.0864	0.2990	0.1005	0.350
1.9	46° 50'	0.1413	0.0655	0.2300	0.0870	0.3067	0.1016	0.360
2.0	48° 17'	0.1486	0.0659	0.2363	0.0877	0.3144	0.1024	0.369
2.1	49° 41'	0.1563	0.0662	0.2410	0.0883	0.3219	0.1032	0.379
2.2	51°	0.1644	0.0664	0.2457	0.0888	0.3298	0.1037	0.389
2.3	52° 17'	0.1730	0.0668	0.2512	0.0891	0.3369	0.1048	0.398
2.4	53° 31'	0.1822	0.0670	0.2567	0.0895	0.3441	0.1053	0.407
2.5	54° 40'	0.1915	0.0671	0.2615	0.0898	0.3515	0.1058	0.416
2.6	55° 46'	0.2013	0.0673	0.2670	0.0902	0.3588	0.1064	0.425
2.7	56° 51'	0.2119	0.0674	0.2725	0.0905	0.3660	0.1071	0.434
2.8	57° 50'	0.2224	0.0675	0.2767	0.0908	0.3739	0.1074	0.443
2.9	58° 49'	0.2337	0.0675	0.2816	0.0910	0.3807	0.1078	0.452
3.0	59° 44'	0.2454	0.0676	0.2863	0.0912	0.3875	0.1082	0.461

TABLE 1—continued

$\beta = 8^\circ$

J	$\phi$	2 Blades		3 Blades		4 Blades		
		$w_c$	$sk_L$	$k_T$	$sk_L$	$k_T$	$sk_L$	$k_T$
0	8°	0.0984	0.0376	0.1086	0.0379	0.1113	0.0382	0.1126
0.05	9° 18'	0.0988	0.0424	0.1218	0.0444	0.1434	0.0451	0.1474
0.1	10° 36'	0.0992	0.0472	0.1357	0.0499	0.1736	0.0511	0.1787
0.15	11° 54'	0.0998	0.0516	0.1482	0.0555	0.2012	0.0570	0.2022
0.2	13° 12'	0.1005	0.0555	0.1588	0.0607	0.2250	0.0622	0.2375
0.25	14° 29'	0.1013	0.0587	0.1675	0.0660	0.2453	0.0681	0.2626
0.3	15° 46'	0.1022	0.0620	0.1768	0.0705	0.2610	0.0727	0.2840
0.35	17° 3'	0.1032	0.0647	0.1845	0.0749	0.2747	0.0782	0.3038
0.4	18° 18'	0.1043	0.0672	0.1917	0.0788	0.2883	0.0829	0.3215
0.45	19° 34'	0.1056	0.0693	0.1978	0.0823	0.2999	0.0871	0.3370
0.5	20° 48'	0.1069	0.0712	0.2038	0.0853	0.2453	0.0913	0.2626
0.55	22° 3'	0.1084	0.0730	0.2100	0.0880	0.2610	0.0948	0.2840
0.6	23° 15'	0.1099	0.0743	0.2136	0.0905	0.2747	0.0981	0.3038
0.65	24° 27'	0.1116	0.0756	0.2182	0.0927	0.2883	0.1017	0.3215
0.7	25° 39'	0.1134	0.0766	0.2214	0.0946	0.2999	0.1047	0.3370
0.75	26° 49'	0.1154	0.0772	0.2242	0.0968	0.2883	0.1078	0.3215
0.8	27° 59'	0.1174	0.0780	0.2270	0.0988	0.2883	0.1101 <sub>b</sub>	0.3215
0.85	29° 7'	0.1196	0.0787	0.2306	0.1004	0.2999	0.1125	0.3370
0.9	30° 15'	0.1219	0.0794	0.2330	0.1019	0.2999	0.1149	0.3370

0.95	31° 20'	0.1243	0.0798	0.2362	0.1033	0.3113	0.1166	0.3506
1.0	32° 27'	0.1269	0.0805	0.2392	0.1046	0.3221	0.1183	0.3650
1.1	34° 34'	0.1323	0.0816	0.2452	0.1070	0.3306	0.1217	0.3791
1.2	36° 37'	0.1383	0.0826	0.2507	0.1088		0.1247	0.3919
1.3	38° 36'	0.1449	0.0839	0.2583			0.1271	
1.4	40° 29'	0.1519	0.0847	0.2633			0.1292	0.4031
1.5	42° 18'	0.1595	0.0857	0.2707			0.1314	0.4163
1.6	44° 3'	0.1677	0.0864	0.2767			0.1334	0.4288
1.7	45° 42'	0.1763	0.0871	0.2833			0.1349	0.4402
1.8	47° 19'	0.1858	0.0878	0.2902			0.1365	0.4523
1.9	48° 50'	0.1957	0.0882	0.2956				
2.0	50° 17'	0.2061	0.0887	0.3017				
2.1	51° 41'	0.2173	0.0891	0.3077				
2.2	53° 0'	0.2290	0.0895	0.3137				
2.3	54° 17'	0.2415	0.0897	0.3198				
2.4	55° 31'	0.2548	0.0900	0.3253				
2.5	56° 40'	0.2685	0.0901	0.3306				
2.6	57° 46'	0.2828	0.0902	0.3356				
2.7	58° 51'	0.2984	0.0904	0.3423				
2.8	59° 50'	0.3138	0.0905	0.3472				
2.9	60° 49'	0.3306	0.0906	0.3520				
3.0	61° 44'	0.3479	0.0907	0.3575				



TABLE 1—continued

$\beta = 10^{\circ}$

J	$\phi$	2 Blades			3 Blades			4 Blades		
		$\alpha^{\circ}$	$sk_L$	$k_T$	$sk_L$	$k_T$	$sk_L$	$k_T$	$sk_L$	$k_T$
0	10°	0.1234	0.0568	0.1614	0.0596	0.1696	0.0601	0.1715	0.0680	0.2124
0.05	11° 18'	0.1240	0.0621	0.1753	0.0661	0.2065	0.0751	0.2501	0.0732	0.2850
0.1	12° 36'	0.1247	0.0674	0.1900	0.0732	0.2397	0.0825	0.3129	0.0797	0.3431
0.15	13° 54'	0.1255	0.0720	0.2027	0.0797	0.2470	0.0887	0.3431	0.0858	0.3850
0.2	15° 12'	0.1265	0.0762	0.2142	0.0858	0.2543	0.0957	0.4129	0.0916	0.4431
0.25	16° 29'	0.1277	0.0798	0.2238	0.0916	0.2603	0.0968	0.4431	0.0957	0.4850
0.3	17° 46'	0.1288	0.0829	0.2318	0.0968	0.2646	0.1015	0.5129	0.1017	0.5431
0.35	19° 3'	0.1302	0.0858	0.2397	0.1017	0.2682	0.1057	0.5431	0.1057	0.5850
0.4	20° 18'	0.1317	0.0884	0.2470	0.1057	0.2713	0.1093	0.5850	0.1093	0.6129
0.45	21° 34'	0.1334	0.0909	0.2543	0.1093	0.2743	0.1116	0.6129	0.1116	0.6431
0.5	22° 48'	0.1352	0.0929	0.2603	0.1116	0.2773	0.1120	0.6431	0.1120	0.6750
0.55	24° 3'	0.1372	0.0946	0.2646	0.1120	0.2819	0.1120	0.6750	0.1120	0.7050
0.6	25° 15'	0.1393	0.0957	0.2682	0.1120	0.2849	0.1120	0.7050	0.1120	0.7350
0.65	26° 27'	0.1415	0.0967	0.2713	0.1120	0.2880	0.1120	0.7350	0.1120	0.7650
0.7	27° 39'	0.1440	0.0976	0.2743	0.1120	0.2910	0.1120	0.7650	0.1120	0.7950
0.75	28° 49'	0.1465	0.0983	0.2773	0.1120	0.2940	0.1120	0.7950	0.1120	0.8250
0.8	29° 59'	0.1493	0.0993	0.2819	0.1120	0.2970	0.1120	0.8250	0.1120	0.8550
0.85	31° 7'	0.1522	0.1001	0.2849	0.1120	0.3000	0.1120	0.8550	0.1120	0.8850
0.9	32° 15'	0.1553	0.1008	0.2880	0.1120	0.3030	0.1120	0.8850	0.1120	0.9150

0.95	33° 20'	0.1584	0.1015	0.2911
1.0	34° 27'	0.1619	0.1024	0.2952
1.1	36° 34'	0.1692	0.1037	0.3014
1.2	38° 37'	0.1772	0.1052	0.3083
1.3	40° 36'	0.1859	0.1063	0.3147
1.4	42° 29'	0.1953	0.1072	0.3212
1.5	44° 18'	0.2055	0.1081	0.3276
1.6	46° 3'	0.2166	0.1091	0.3353
1.7	47° 42'	0.2282	0.1098	0.3413
1.8	49° 19'	0.2410	0.1105	0.3481
1.9	50° 50'	0.2543	0.1112	0.3549
2.0	52° 17'	0.2685	0.1116	0.3612
2.1	53° 41'	0.2838	0.1121	0.3670
2.2	55° 0'	0.2996	0.1123	0.3728
2.3	56° 17'	0.3168	0.1123	0.3782
2.4	57° 31'	0.3350	0.1130	0.3849
2.5	58° 40'	0.3539	0.1132	0.3906
2.6	59° 46'	0.3737	0.1134	0.3959
2.7	60° 51'	0.3952	0.1136	0.4012
2.8	61° 50'	0.4168	0.1138	0.4073
2.9	62° 49'	0.4401	0.1139	0.4124
3.0	63° 44'	0.4643	0.1139	0.4164

TABLE I--continued

 $\beta = 12^\circ$ 

J	$\phi$	$w_c$	2 Blades		3 Blades		4 Blades	
			$sk_L$	$k_T$	$sk_L$	$k_T$	$sk_L$	$k_T$
0	12°	0.1488	0.0787	0.2186	0.0847	0.2430	0.0870	0.2426
0.05	13° 18'	0.1496	0.0844	0.2332	0.0928	0.2576	0.0955	0.2651
0.1	14° 36'	0.1505	0.0897	0.2472	0.1002	0.2769	0.1039	0.2871
0.15	15° 54'	0.1517	0.0944	0.2593	0.1074	0.2959	0.1119	0.3084
0.2	17° 12'	0.1530	0.0982	0.2684	0.1142	0.3135	0.1196	0.3282
0.25	18° 29'	0.1544	0.1020	0.2796			0.1264	0.3464
0.3	19° 46'	0.1561	0.1057	0.2892			0.1330	0.3639
0.35	21° 3'	0.1579	0.1084	0.2958				
0.4	22° 18'	0.1599	0.1110	0.3020				
0.45	23° 34'	0.1621	0.1131	0.3083				
0.5	24° 48'	0.1644	0.1148	0.3127				
0.55	26° 3'	0.1670	0.1159	0.3160				
0.6	27° 15'	0.1697	0.1171	0.3197				
0.65	28° 27'	0.1726	0.1186	0.3236				
0.7	29° 39'	0.1757	0.1198	0.3270				
0.75	30° 49'	0.1790	0.1207	0.3298				
0.8	31° 59'	0.1826	0.1218	0.3333				
0.85	33° 7'	0.1863	0.1227	0.3370				

TABLE 2

Table of values of  $sk_L$  and  $k_T$  for given values of  $J$  and for  $\alpha = 0.7$  for 6 blades and infinity blades.

$\beta^\circ$	$2^\circ$				$4^\circ$			
	6 Blades		Infinity Blades		6 Blades		Infinity Blades	
No. of blades	$sk_L$	$k_T$	$sk_L$	$k_T$	$sk_L$	$k_T$	$sk_L$	$k_T$
J								
0	0.0024	0.0071	0.0024	0.0071	0.0096	0.0285	0.0096	0.0289
0.1	0.0056	0.0168	0.0056	0.0168	0.0160	0.0470	0.0161	0.0474
0.2	0.0088	0.0262	0.0088	0.0262	0.0223	0.0658	0.0224	0.0660
0.3	0.0117	0.0353	0.0118	0.0355	0.0284	0.0839	0.0285	0.0842
0.4	0.0149	0.0450	0.0149	0.0450	0.0342	0.1012	0.0345	0.1021
0.5	0.0176	0.0537	0.0178	0.0543	0.0400	0.1195	0.0404	0.1207
0.6	0.0203	0.0627	0.0207	0.0637	0.0449	0.1345	0.0461	0.1382
0.7	0.0228	0.0711	0.0235	0.0733	0.0498	0.1510	0.0516	0.1564
0.8	0.0252	0.0795	0.0261	0.0823	0.0541	0.1655	0.0568	0.1738
0.9	0.0273	0.0876	0.0287	0.0921	0.0578	0.1790	0.0619	0.1917
1.0	0.0291	0.0948	0.0311	0.1013	0.0612	0.1920	0.0667	0.2092
1.1	0.0307	0.1002	0.0334	0.1092	0.0641	0.2042	0.0711	0.2263
1.2	0.0321	0.1063	0.0355	0.1177	0.0667	0.2154	0.0754	0.2436
1.3	0.0333	0.1122	0.0376	0.1267	0.0689	0.2262	0.0794	0.2606
1.4	0.0344	0.1183	0.0395	0.1363	0.0711	0.2367	0.0832	0.2768
1.5	0.0354	0.1242	0.0413	0.1449	0.0731	0.2485	0.0867	0.2948
1.6	0.0363	0.1301	0.0430	0.1541	0.0747	0.2590	0.0900	0.3123
1.7	0.0372	0.1361	0.0446	0.1632	0.0764	0.2697	0.0930	0.3285
1.8	0.0379	0.1415	0.0461	0.1721	0.0777	0.2791	0.0960	0.3450
1.9	0.0386	0.1470	0.0474	0.1803	0.0790	0.2896	0.0986	0.3615
2.0	0.0392	0.1527	0.0487	0.1897	0.0801	0.2990	0.0986	0.3615
2.1	0.0398	0.1580	0.0499	0.1980	0.0810	0.3086	0.0986	0.3615
2.2	0.0402	0.1630	0.0510	0.2068	0.0819	0.3173	0.1012	0.3776
2.3			0.0521	0.2156				
2.4			0.0531					



TABLE 3

Values of  $k_L$  and  $k_D$  at  $x = 0.7$  deduced from analysis of performance data of actual model airscrews :—R.A.F. 6 type sections ; Ref. 4 ; standard 2 bladers (Figs. 8 and 9) and 4 bladers ; also mean of 2 and 4 blades.

Range of pitch ratio 0.3 to 2.5.

$\alpha^\circ$	2 Blades		4 Blades		Mean of 2 and 4 Blades	
	$k_L$	$k_D$	$k_L$	$k_D$	$k_L$	$k_D$
—4.4	0	0.0212				
—4.25			0	0.0208		
—4.0	0.026	0.0183	0.017	0.0194	0.021	0.0187
—3.0	0.087	0.0136	0.081	0.0137	0.084	0.0136
—2.0	0.141	0.0107	0.137	0.0114	0.139	0.0110
—1.0	0.192	0.0091	0.184	0.0102	0.188	0.0096
0	0.239	0.0082	0.230	0.0096	0.235	0.0089
+1	0.283	0.0077	0.273	0.0095	0.278	0.0086
2	0.323	0.0078	0.311	0.0099	0.317	0.0088
3	0.360	0.0083	0.349	0.0107	0.355	0.0095
4	0.399	0.0093	0.385	0.0119	0.392	0.0106
5	0.435	0.0107	0.423	0.0134	0.429	0.0120
6	0.470	0.0123	0.456	0.0152	0.463	0.0137
7	0.503	0.0143	0.492	0.0173	0.497	0.0158
8	0.533	0.0167	0.526	0.0199	0.529	0.0184
9	0.563	0.0199	0.558	0.0230	0.560	0.0215
10	0.587	0.0243	0.590	0.0265	0.588	0.0254
11	0.609	0.0299	0.620	0.0310	0.615	0.0305
12	0.629	0.0370	0.649	0.0370	0.639	0.0370
13	0.642	0.0450	0.660	0.0450	0.651	0.0450
14	0.651	0.0540	0.665	0.0580	0.658	0.0560
15	0.660	0.0660	0.665	0.0730	0.662	0.0695
20	0.688	0.148	0.652	0.158	0.670	0.153
25	0.700	0.252	0.673	0.249	0.686	0.2505
30	0.705	0.357	0.690	0.337	0.697	0.347
35	0.698	0.461				

## LIST OF REFERENCES

1. R. & M. 892. Experiments with a family of airscrews. Part III. Analysis of the family of airscrews by means of the vortex theory.—Lock and Bateman.
2. R. & M. 1377. Application of Goldstein's theory to the practical design of airscrews.—Lock.
3. R. & M. 1152. An application of Prandtl theory to an airscrew.—Lock.
4. R. & M. 1673. Wind tunnel tests of high pitch airscrews.—Lock, Bateman and Nixon.
5. R. & M. 1674. Tables for use in an improved method of airscrew strip theory calculations.—Lock and Yeatman.
6. R. & M. 1086, 1091, 1123, 1124, 1134, 1174, 1198, 1438, etc. Wind tunnel experiments on high tip speed airscrews. Douglas and Perring.

Chart 1;  $sk_L$  against  $\phi$  for given  $J$ . Two bladed airscrews, radius 0.7.

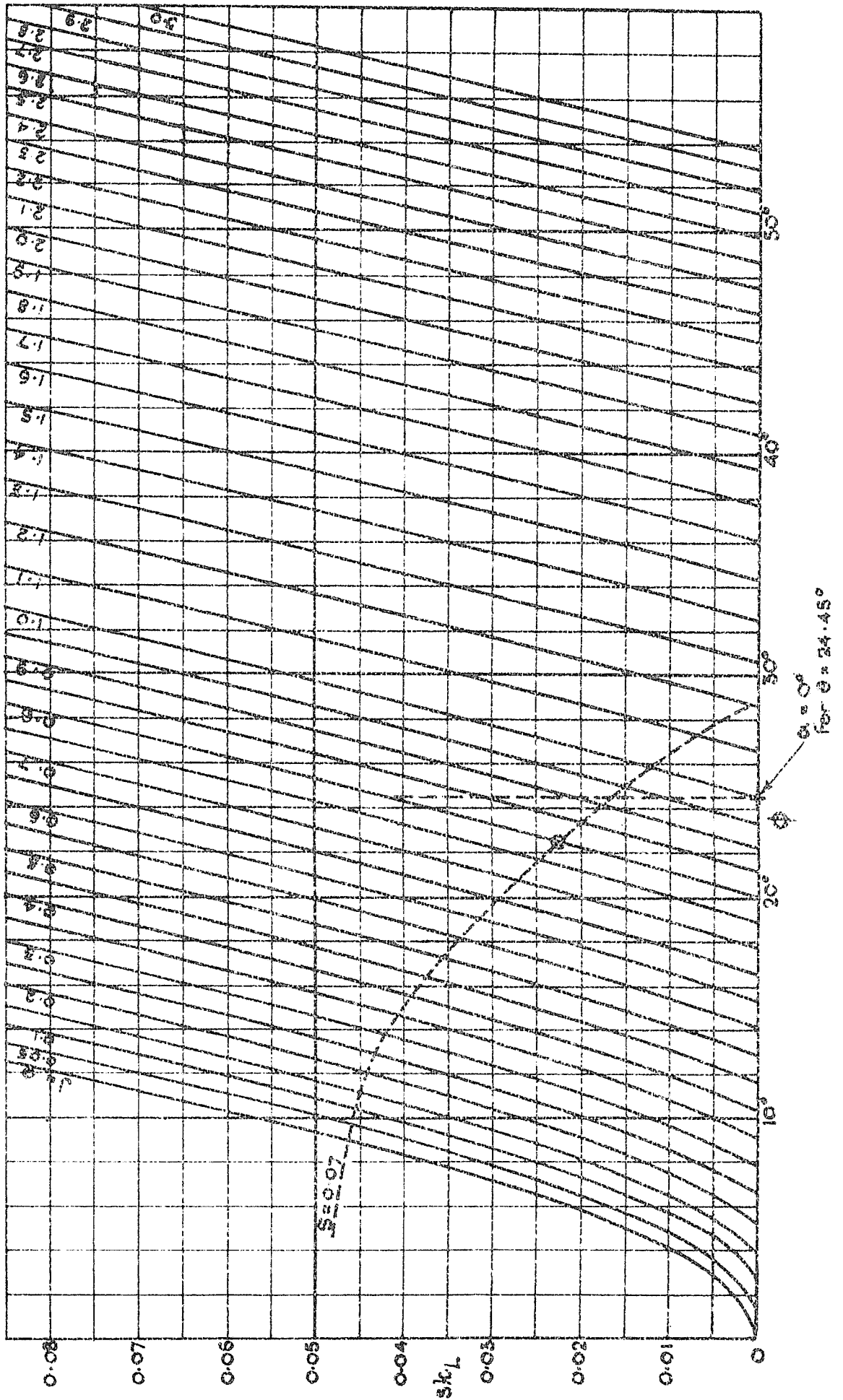




Chart 2;  $sk_L$  against  $\alpha$  for given  $s$  at radius 0.7. (R.A.F. 6 section: table 3)

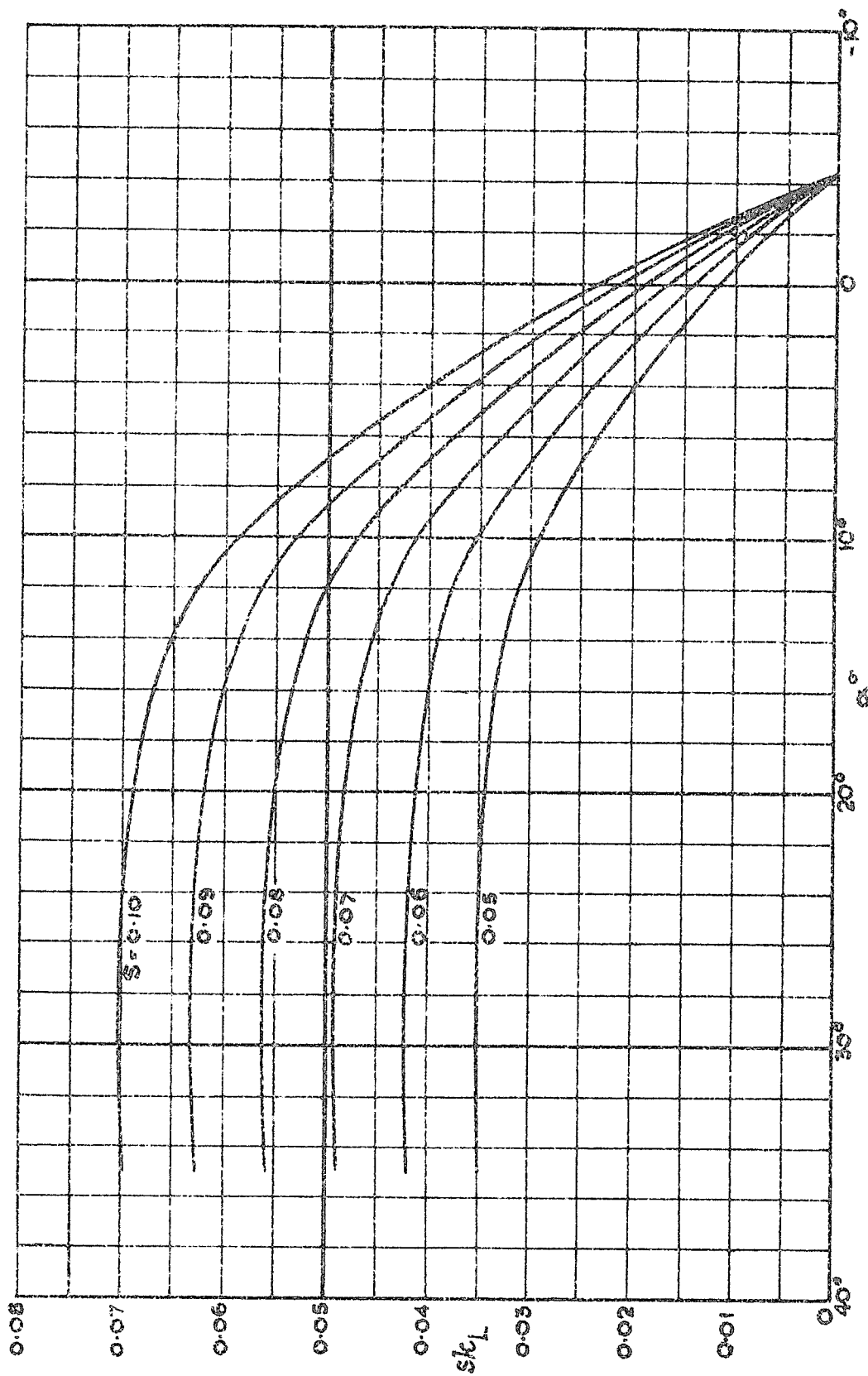


Chart 3;  $k_T$  (or  $\frac{dk_T}{d(x^2)}$ ) against  $sk_L$  for given  $J$ ;  
Two blades; radius 0.7.

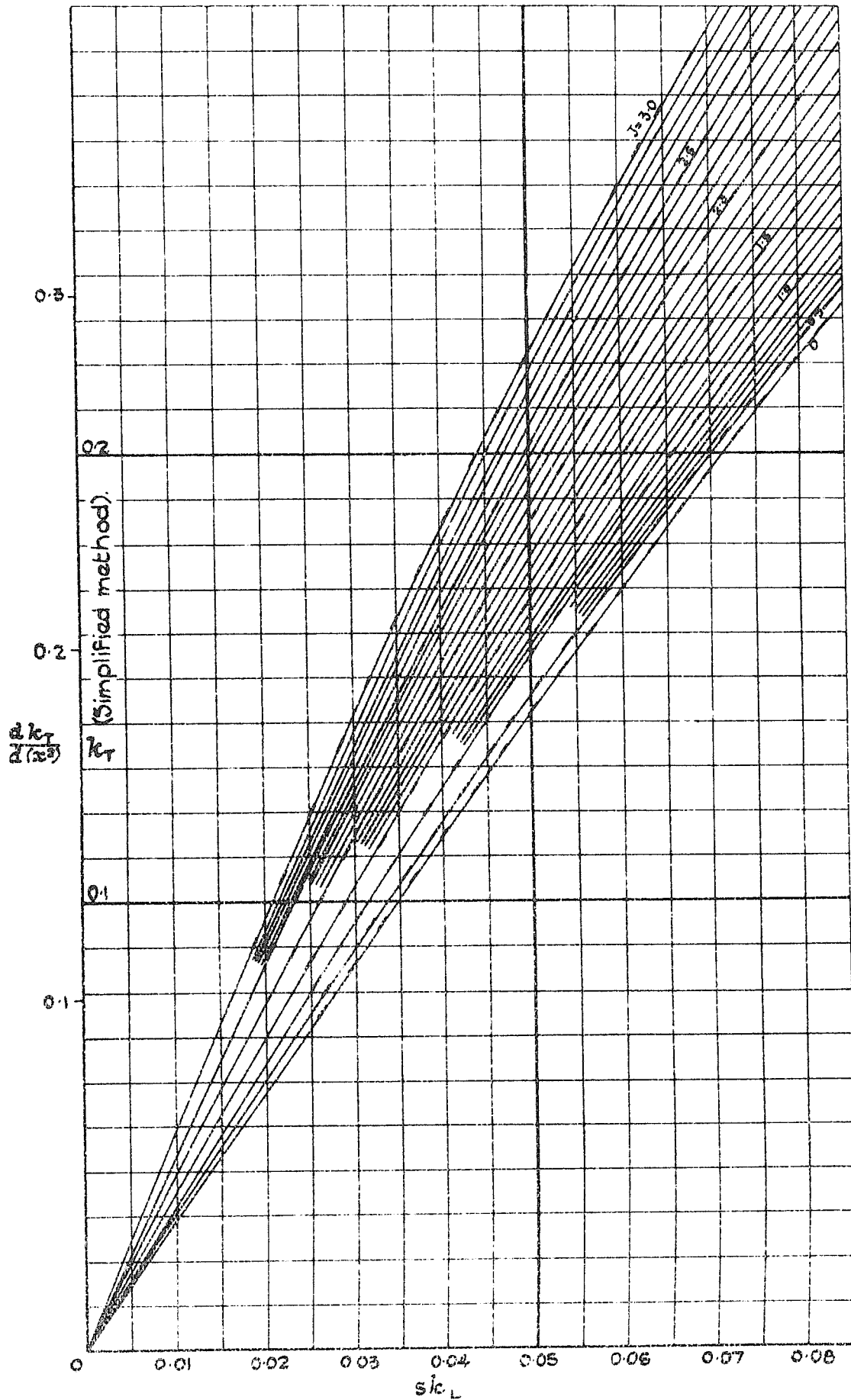


Chart 4;  $w_c$  against  $sk_L$  For given  $J$ .  
Two blades, radius 0.7.

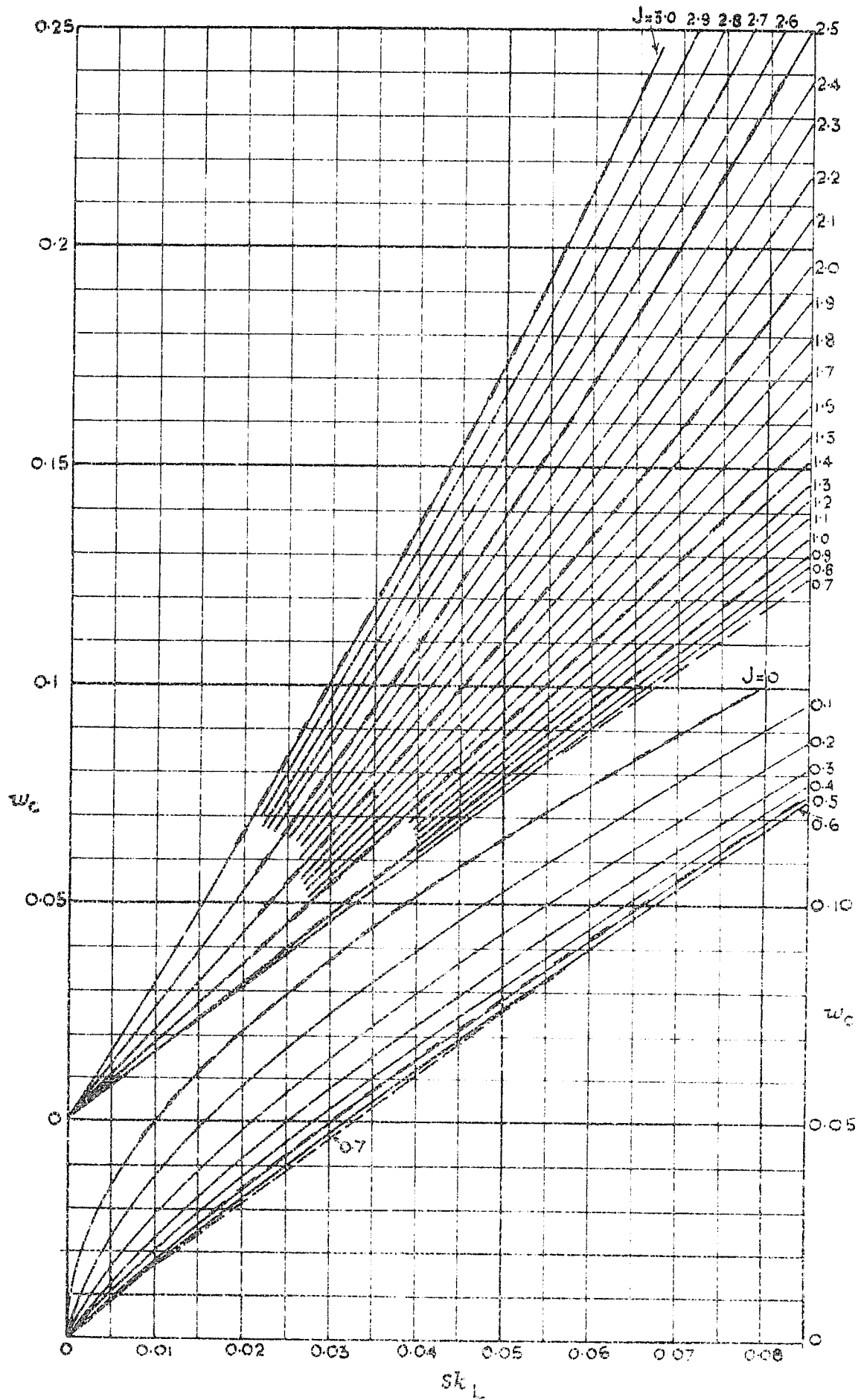


FIG. 7.

Chart 6;  $sk_0$  against  $\alpha$  for given  $s$ ; radius 0.7.  
(R.A.F. 6 section: table 3).

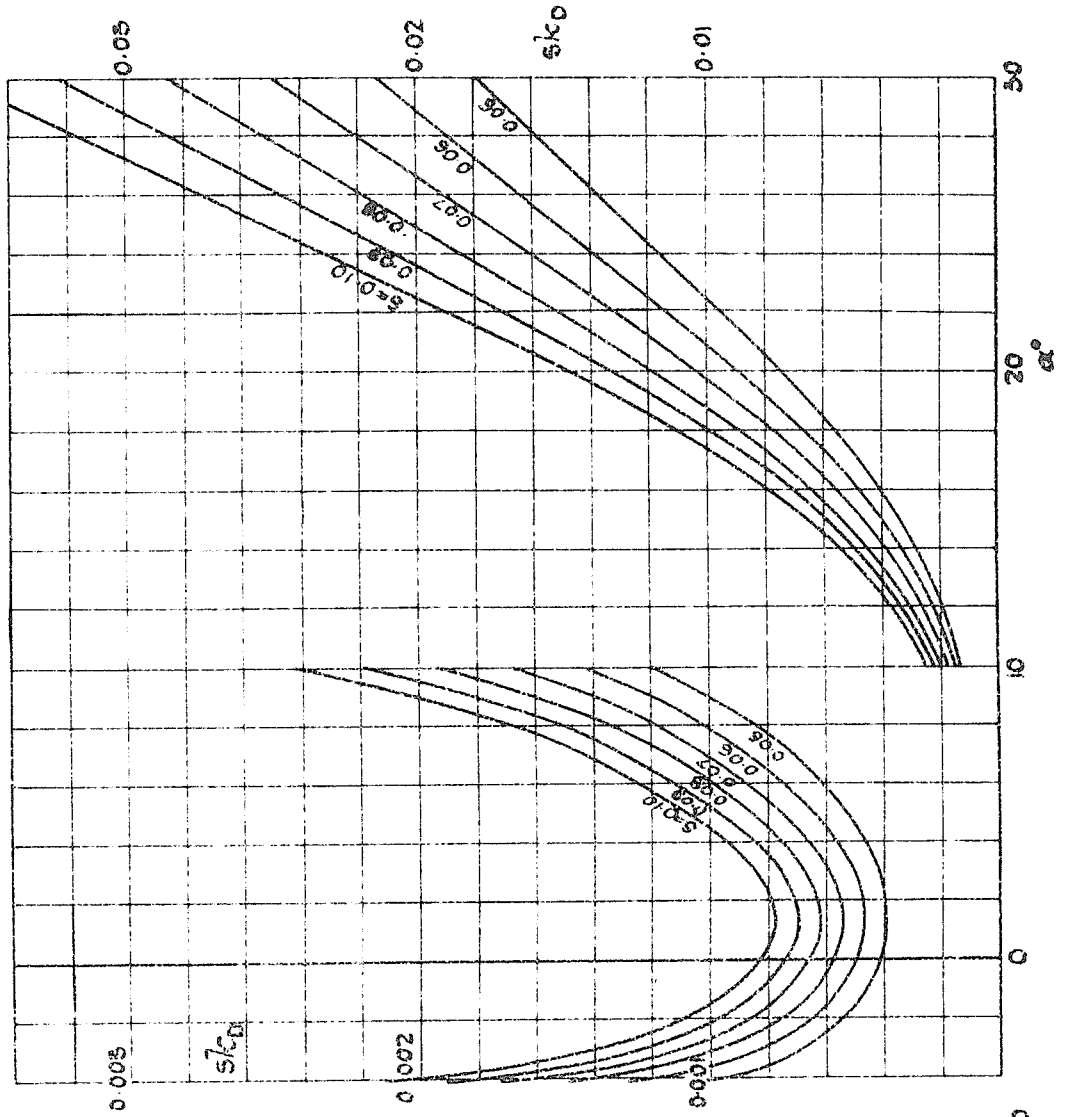
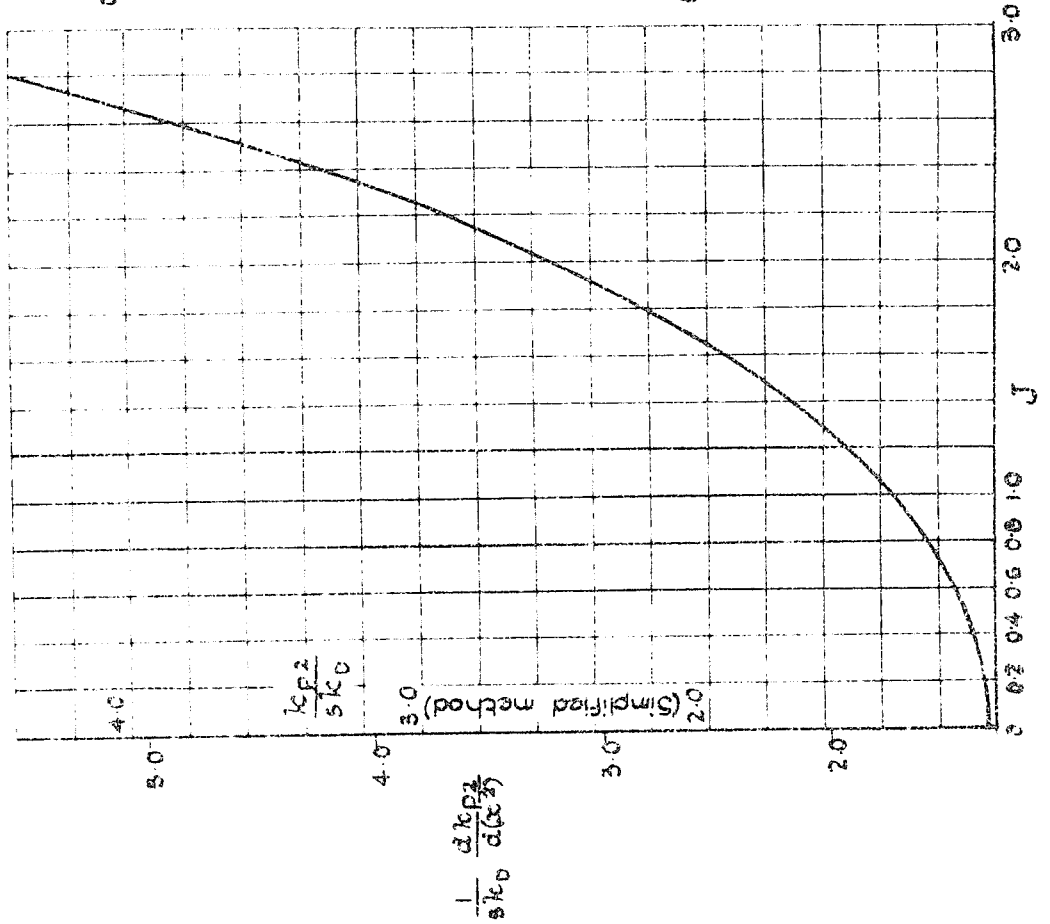
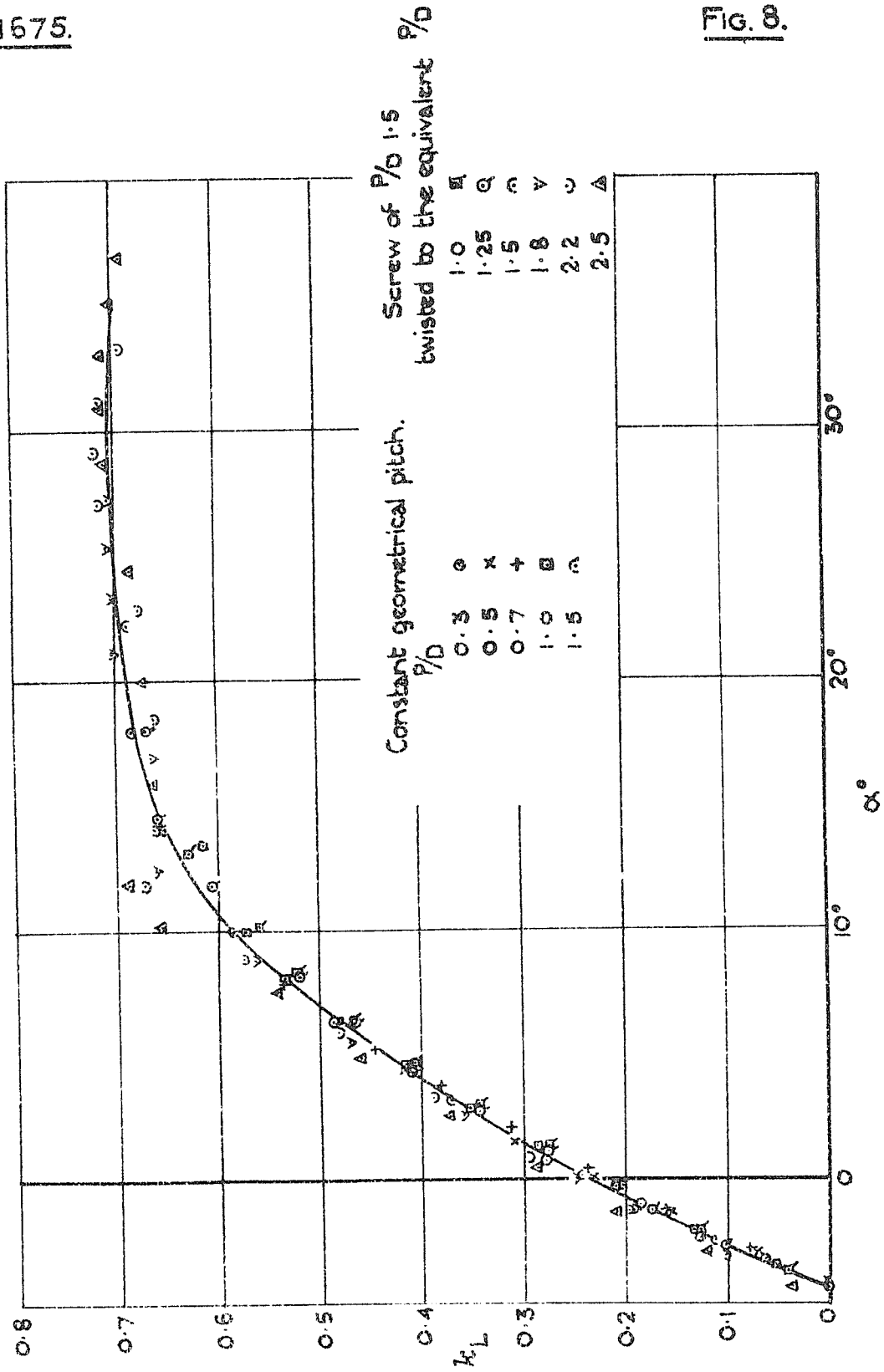


FIG. 6.

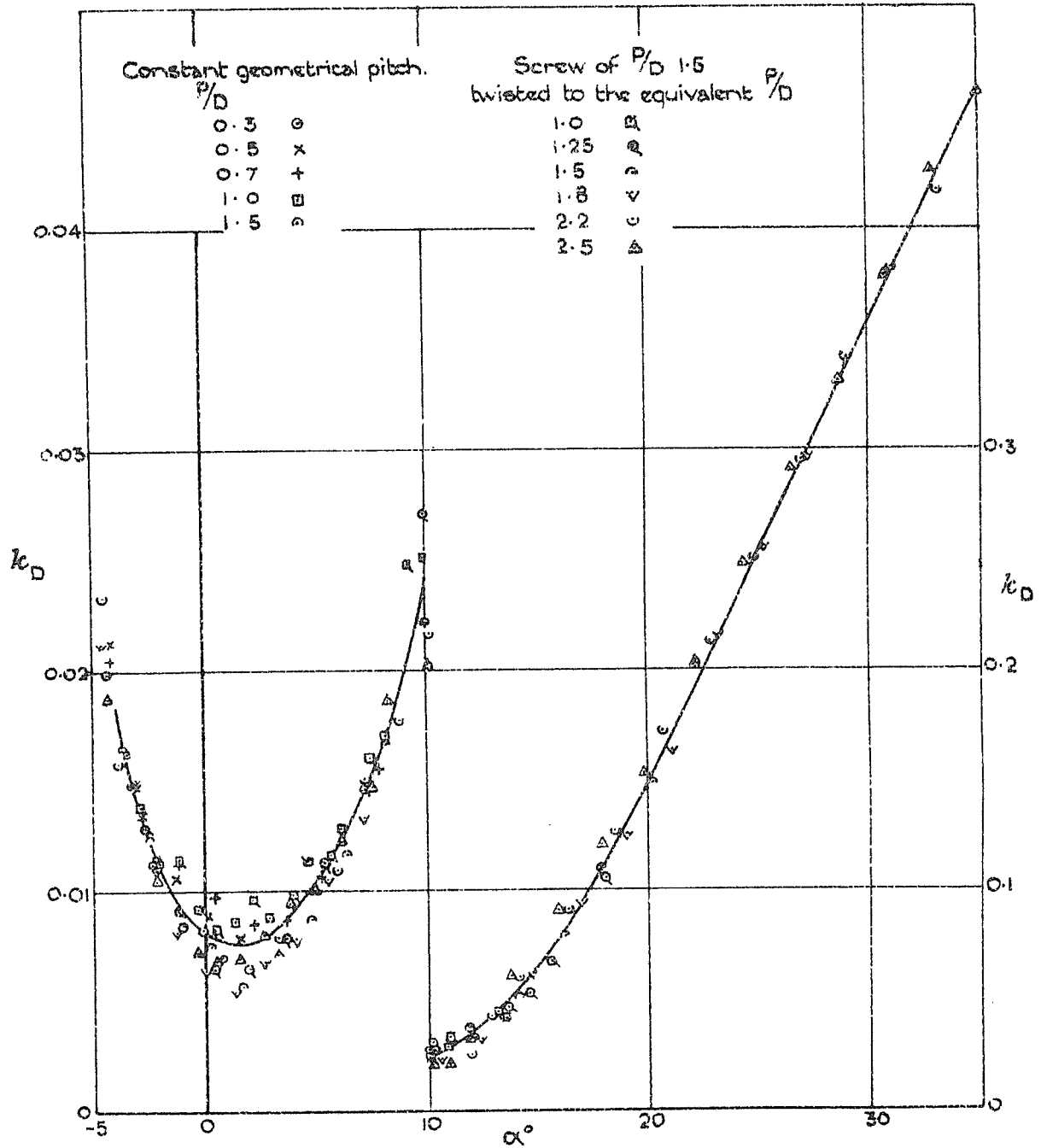
Chart 5; Curve of  $k_{p2}/sk_0$  (or  $1/sk_0$ ) against  $J$ . Radius 0.7.



Analysis of observed performance of model 2 bladed airscrews.  
 Values of  $k_L$  plotted against  $\alpha$  for radius 0.7 derived from  
 airscrews of pitch values as follows.



Analysis of observed performance of model 2 bladed airscrews.  
 Values of  $k_D$  plotted against  $\alpha$  for radius 0.7 derived from  
 airscrews of pitch values as follows.



Lift and Drag Coefficient Curves for a Section at 0.7  
Radius of an Airscrew Blade.

